(To be **submitted to Journal of Physics D: Applied Physics)**

Dual metal-insulator and insulator-insulator switching in nanoscale and Al doped VO_2 above the transition temperature

A. Gentle and G. B. Smith
Institute of Nanoscale Technology: University of Technology, Sydney;
PO Box 123 Broadway NSW 2007Australia

Email: g.smith@uts.edu.au

Abstract

Thin films of VO_2 doped with aluminium, or with nanoscale grain sizes, have been produced. They display semiconductor resistive behaviour above the transition temperature T_c, but metallic and plasmonic optical response. All samples optically switch over almost identical large ranges at the transition, but have quite variable resistive switching. At fixed grain size a rigorous new quantitative correlation is found between semiconductor resistivity below T_c and the activation energy above T_c as Al doping level varies. Large crystals doped with Al also display this dual behaviour. A possible mechanism is discussed involving fast local fluctuations on neighbouring V^{4+} ions involving transient dimers with no net spin. Such fluctuations would then need to interact and correlate their motion over the scale of a nanograin within the lifetime of the dimer excitation.

1. Introduction

The first order phase transition in undoped VO_2 occurs at T_c = 340°K. It is usually assumed to be a metal-insulator transition because the high temperature phase has a lower dc resistivity than the low temperature state by several orders of magnitude, and because it also reflects much more strongly at near infra-red (NIR) wavelengths. However the temperature dependence of resistance at $T > T_c$ can be that of a semiconductor rather than a metal, even though NIR reflectance is high.

In depth analysis of the "metal" phase transport properties in terms of models for classical metal behaviour over a wide frequency range from optical to dc runs into various difficulties. The most prominent issue to date is apparent at both optical frequencies [1-3] and in dc resistance [4]. This is the anomalously high relaxation frequency ω_τ which is in the range 0.65 eV to 1.2 eV [2,4,5], so the relaxation time is very fast at ~3 femtoseconds. Optical data still follows a classical Drude model as expected of a metal at long enough wavelengths, and in most cases plasmonic response is found. For static fields however response for many classes of VO_2 is often not that of a metal but of another semiconductor [2,6]. This feature has rarely been noted and thus has received little attention. If in the same samples optical data is that of a plasmonic metal with no band gap, while dc conductance at T > Tc is thermally activated as if a band gap still exists we cannot simply treat such VO_2 systems as

conventional metals. A new material description is needed consistent with such observations. This study provides both novel contexts and some new characteristics of such mixed character in terms of the effect of dopants and of grain size. Finally we outline how, in terms of electron and hole properties, one might reconcile resistance data that says we have two distinct semiconductors above and below the phase transition, with optical data that says there is a metal-semiconductor transition.

In the quest for an understanding of this dual character electrical, optical and structural data has been acquired on a wide range of samples that exhibit this behaviour. Data above and below T_c is needed since the influences on the "metal" state resistivity also alter electrical properties below T_c. Two important influences have been identified, grain size and impurity doping with aluminium. Doping alters T_c, grain size does not. The change in resistivity as a function of grain size and of Al doping levels will be seen to be quite systematic and wide ranging. In contrast optical data is largely unaffected. Without doping the dual character is only found with nano-grain samples.

Grain size G has a counter intuitive influence in both phases on response to electric fields since we will show smaller G values actually raise conductivity substantially, whereas impurities and a higher density of grain boundaries in normal materials are expected to lower conductivity due to an increased relaxation rate. In metallic VO_2 we find they have little impact on ω_τ, which indicates the anomalously high relaxation rate is intrinsic. At first sight their counter intuitive impact on resistivity implies close grain boundaries appear to raise carrier density. Unlike dopants, which do raise carrier density, smaller grain sizes however do not alter T_c. We return to these dilemmas later in addressing our data. Nanoparticles of normal metals under around 40 to 50 nm in diameter usually have enhanced carrier relaxation rates due to surface collisions, but in small VO_2 nanoparticles this is not an issue [7], again because ω_τ is so high.

As the frequency, ω, of the applied field drops below ~ 0.4eV [8] diverse behaviours arise with structure and doping. The phase change in VO_2 can also be made to occur very quickly [9,10] which indicates ionic movement is playing a secondary role in the phase transition and electron-electron or electron-hole interactions are dominating. Being a much lighter combination they are able to adjust rapidly to both external and internal perturbations. In contrast to the wide range of resistivity switching amplitudes we will demonstrate that the NIR switching amplitude for reflectance or transmittance is barely affected by Al doping levels or grain size. To enhance our understanding of this novel state at $T > T_c$ we have thus carried out a systematic experimental study of dc and NIR properties using different Al doping levels and grain sizes.

2. Electrical and optical properties

The temperature dependence of resistivity in thin film samples with grain sizes under around 200 nm, both doped with aluminium and undoped, provides a good basis for characterising key aspects of the dual character. The activation energy ΔE_m for dc conductivity at $T > T_c$ is contained in equation 1(a). (We use resistivity to facilitate comparisons with most other data on VO_2 in the literature). ΔE_m is much lower than ΔE_{sc} the activation energy in the semiconductor state given in equation 1(b). However ΔE_m and ΔE_{sc} are not independent, and both depend on dopant concentration c. We

will demonstrate this by tracking the link between resistivity at $T < T_c$ and at $T > T_c$ as the level of aluminium doping changes at fixed grain size.

$$\rho_m(T,c) = \rho_{0,sm}(c)e^{[\Delta E_m(c)/kT]} \qquad T > T_c \quad (1a)$$

$$\rho_{sc}(T,c) = \rho_{0,sc}(c)e^{[\Delta E_{sc}(c)/kT]} \qquad T < T_c \quad (1b)$$

Dopants have been the focus of many studies on lowering T_C [13]. While a fall in T_C also occurs in this study, we focus on metal phase response. Our T_C values in the samples reported here range from 68°C to 50°C.

Even single crystals can be insulating rather than metallic in dc experiments above T_C provided they are doped, as first noticed many years ago for select dopants by MacChesney and Guggenheim [6]. This peculiarity seems to have been ignored until recently [2]. Checks of optical properties above T_C to see if they were metal or semiconductor like, was apparently not done at that time. Our samples display metal like optical response with no evidence of a different permanent band gap, which even if small should impact on optical data. The original assumption [6] was thus that the transition in these types of doped samples was from one semiconductor state to another with a smaller band gap. That is there was also a permanent band gap above T_c. The "gap" we observe in the thermally activated dc response cannot be interpreted this way if it is not present in optical data and is found only in specific structures. One explanation is that the "gap" seen in dc experiments is not fixed in time with its characteristic lifetime determining whether it is observable at a particular frequency. How such a dynamic gap might originate is considered later.

We now consider doping with Al in detail. The most promising dopants in VO_2 raise carrier densities and conductivity at $T < T_c$, but the process is believed to be different to that in normal semiconductor doping. The dopants used here in common with some interfaces [5], appear to alter local V-V dimer spacings and hence reduce local energy level spacings to facilitate thermal activation of carriers. The very existence of the permanent gap below T_c, and its magnitude, is now known to depend on the strength of the electron correlations [14] within and between singlet V dimer pairs. In VO_2 valence band holes in the low T state can trigger the transition since they weaken the net electron-electron repulsion. The critical hole value is estimated to be 0.018% [15] and can be achieved by raising T, doping, band bending, and with optical pumping [9,10].

Our undoped thin film preparation conditions involved V metal sputter deposition and subsequent controlled oxidation, and are described in reference [2]. Example micrographs showing the various average nano-grain sizes appear in figure 1. Process and substrate changes enabled alteration and control of grain size in the range 30 nm to 100 nm. For doping we co-deposit various amounts of Al_2O_3 via rf sputtering. Varying aluminium dopant concentration c at fixed grain size, modulates both ΔE_m and ΔE_{sc} and hence the switching range for resistivity, in a well defined way while T_C also shifts continuously. In contrast the amplitude of the switch in spectral transmittance and reflectance at optical frequencies above and below T_C are barely affected even though T_C falls as c rises. Sets of optical switching hysteresis curves appear in figure 2 and contrast with the changes in switching amplitude for resistivity

switching in figure 3. Table 1 lists some of the dc activation energies. It includes results for our nano-grain samples with and without Al doping, and some extracted from the data in reference [6] for Al doped and undoped single crystals. ΔE_m and ΔE_{sc} generally fall as c rises at fixed grain size as expected if hole concentration is increasing. In the absence of doping ΔE_{sc} has a maximum around 455 meV in single crystals and large grains, but is lower at ~300 meV in the nanograin films in this study. Doping lowers it further with values as low as 80 meV in our most heavily doped samples. This implies a continual change in band structure with doping concentration c. A gradual weakening of the local Coulomb interaction is thus induced as doping levels increase. Shifts in band energies and densities of states then follow.

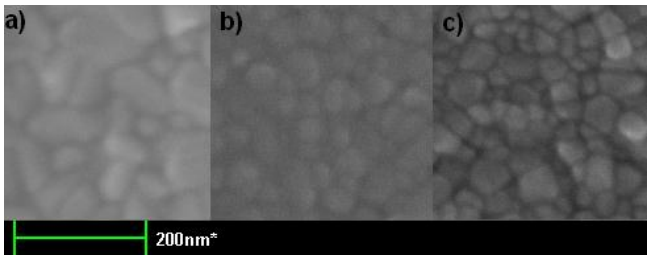

Figure 1 - Scanning electron micrographs of a) 120nm of VO2 on mica - 100nm average grain size b) 50nm of VO2 on glass - 50nm average grain size. c) An example of 50nm thick VO2:Al

Table 1. Activation energies with and without Al dopants.

Samples	ΔE_{sc} (meV)	ΔE_m (meV)	Grain size (nm) [a]
(a) Single crystal [6]			
Undoped	455	absent	large
0.24% Al	380	196	large
0.49% Al	238	119	large
(b) Nanoscale grains			
Undoped	304	50	100
Undoped	165	109	50
Al doped -1	241	89	50
Al doped-2	224	58	50
Al_2O_3 substrate	281	164	50

[a] Variation ± 10 nm

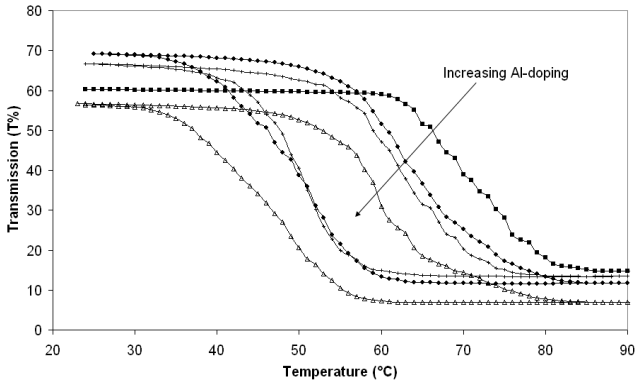

Figure 2 - Optical hysteresis of transmission at 2500nm, for varied Al-doping.

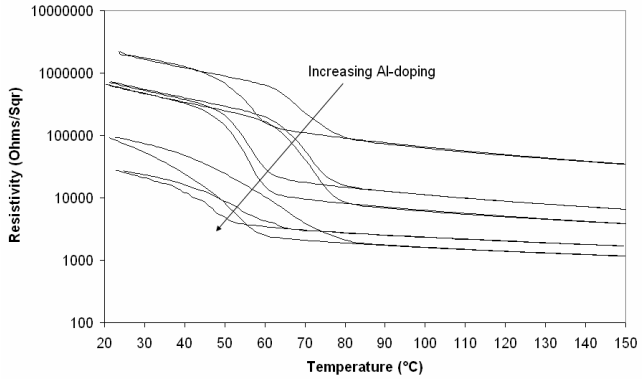

Figure 3 - Electrical resistivity hysteresis for varied Al-doping.

3. A novel link between data above and below T_c

We now present a striking new result which shows that semiconductor carrier density induced by doping, and the strength of the high temperature activation energy are strongly correlated. The variation of ΔE_m for a fixed grain size as plotted in figure 4, follows a universal curve as a function of semiconductor resistivity. This curve is given by equation (2) with A = 0.0089 Ω□cm and β□= 0.043 meV^{-1}. In addition to the role of grain size two other special features stand out (i) the fitting parameter β is close to $1/[kT_r]$ with T_r the temperature at which the semiconductor data was obtained. If we assume β□= 1/kT we get T = 260°K which is a little lower than T_r (ii) a point which was obtained in an entirely different way by depositing a film of the same grain size on an alumina substrate lies exactly on this curve, but well up. This film has the largest ΔE_m value, is our most insulating, and has the smallest switching range for static fields, yet optically it switches fully like good quality normal VO_2.

$$\rho_{sc}(T_r, c) = Ae^{\beta \Delta E_m(c)} \quad (2)$$

Another point is plotted in figure 4 which lies well off this curve. It is for an undoped film with a much different grain size of ~100 nm and has ΔE_m = 63 meV. It is there to highlight the importance of G to these high T anomalies and also demonstrates that for a fixed value of ΔE_m doubling grain size causes semiconductor resistivity to jump by nearly an order of magnitude. Others have recently reported a similar impact of grain size on semiconductor resistivity [16].

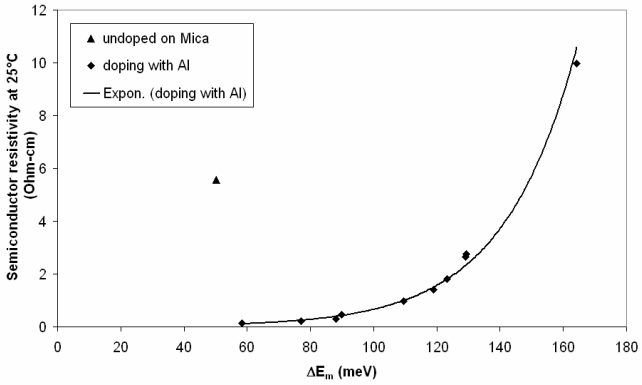

Figure 4 - Room temperature semiconductor resistivity vs metallic state activation energy.

We have results so far on films covering three average grain sizes under 100 nm. The indications are that ΔE_m scales linearly with grain size G at fixed Al dopant levels. Extrapolation of this line yields a maximum value of ΔE_m ~ 150 meV when there is no Al doping, with a maximum grain size above which the dc resistance will be metallic with no Al doping of ~180 nm. From table 1, ΔE_m is approximately half ΔE_{sc} for large grain samples which are doped.

4. Discussion

Drawing all of these observations together a number if questions arise. What is behind the existence of these anomalous low frequency properties, especially the high temperature activation energy ΔE_m? What can happen in a highly correlated electronic system at small grain size, but not in large crystal sizes? Why does Al doping level c link the two activation energies in such a well defined and simple manner at fixed average grain size, while also "turning on" the apparent semiconductor resistive response in large crystals? Scale in space and time are clearly both playing a role. The excitations involved we assume are those that are frozen in below T_c but are transient above T_c. These are singlet pairings on V-V dimers [14] and should be transient above T_c. But local fluctuations would be expected to increase not decrease resistivity and to cause an observable band gap implies that such fluctuations can become coherent on a finite scale in these samples. To explain the observed dual character the time scale of such coherence has to be short enough so that at low enough frequencies they appear to be always "on" but at optical frequencies they are not seen. Coherence also means local fluctuations are in phase and interacting. The need for nanosize grains may be linked to their ability to stabilise this coherence over small enough scales, while incoherence is more likely as scale increases as found in large grain samples.

A schematic of the basic dimer pair structures [14] above and below T_C for undoped large grain samples is in figure 5 as an aid to understanding these excitations. Only V^{4+} involved in σ-bonds are shown explicitly and these align along the c-axis. All eight V^{4+} ions forming the π-bonds with each ion are not shown explicitly, just four for simplicity. Bonding orbitals are represented by solid lines and anti-bonding and empty orbitals by dashed lines. A strong intra-dimer link between singlet electron pairs (and holes) is illustrated in the semiconductor state, while bonding and anti-bonding inter-dimer bonds and unoccupied π-bonds lead to the low T band gap. Above T_C in the metal state electrons can move approximately equally easily [14] along bonds of both types which are all occupied. Transient formation of a single non-

magnetic dimer pair and a coherent array of such pairs within the metal as might explain our optical and resistance data are also shown in figure 5. The V-V spacing must play a crucial role and may be altered by doping and interfaces. It is interesting to note that excitons have long been of interest for high temperature coherence and that "artificial" exciton coherence involving separate layers of electrons and holes in a magnetic field has been achieved [12]. In that case layer spacing was also important. Each dimer could be considered to be a coupled non-magnetic pair of excitons at $T > T_c$. A very fast interaction mechanism between dimer pairs is needed to create this high T coherence [11] and may be possible in such a highly correlated electron-hole system.

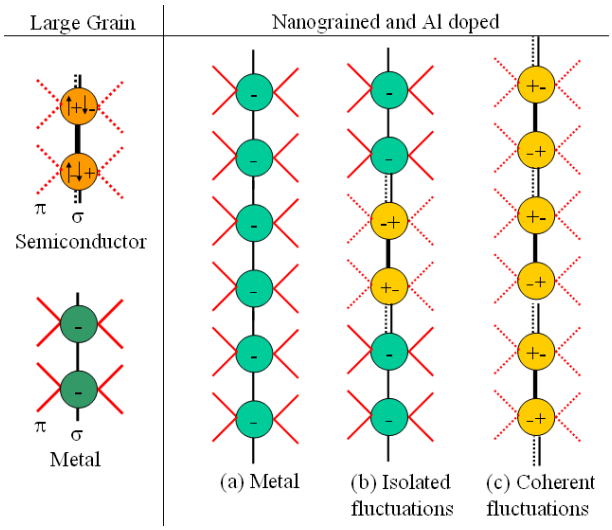

Figure 5 - Schematic of bonding and local spins for large grain samples above and below T_c, and for nanograined and Al doped VO_2 above T_c.

Two final issues from the data are worth comment. The first concerns the observation that doping can switch on the "transient semiconductor state" even in single crystal samples. The distance between dopants may play a similar role to the separation between grain boundaries in defining a coherence scale. This points to defects and grain boundaries both acting to "pin" the transient phase. The second issue concerns empirical data equation (2). It appears to be a universal curve for a fixed grain size as carrier density changes, with its left hand side given by equation (1b). The right hand side however is not equation (1a) since A is universal, being independent of c though the fact $1/\beta$ □is close to kT_r is surprising. Further analysis of our experimental R vs T data clearly shows that $\rho_{0,sc}$ varies significantly and systematically with c. The density of states near the gap plays a role in this term and understanding the impact of c on density of states should add to our understanding of this link between the fixed and transient semiconductor states in this very unconventional material. This is under study. Dynamic experiments especially at femtosecond time scales, or even faster are needed to fully understand this dual state.

Acknowledgements

We would like to thank Abaas Maaroof, Geoff McCredie and Mike Cortie for their input into this work.

References

[1] Veleur, H.A., Barker, A.S. & Berglund, C.N., Optical Properties of VO_2 between 0.25 eV and 5 eV *Phys. Rev.* **172** 788-798 (1968)

[2] Gentle, A., Maaroof, A.I. & Smith, G.B., Nanograin VO_2 in the metal phase: a plasmonic system with falling dc resistivity as temperature rises. *Nanotechnology* **18**, 025202(7pp) (2007).

[3] Choi, H.S., Ahn, J.S., Jung, J.H. & Noh, T.W. Mid-infra-red properties of a VO_2 film near the metal-insulator transition *Phys. Rev. B* **54** 4621 4628 (1996)

[4] Allen, P.B., Wentzcovitch, R.M. & Schultz, W.W., Resistivity of the high-temperature metallic phase of VO_2 *Physical Review B* **48** 4359-4363 (1993)

[5] Okazaki, K., Sugai, S., Muraoka, Y. & Hiroi, Z., Role of electron-electron and electron-phonon interaction in optical conductivity of VO_2 *Physical Review B* **73** 165116, 1-5 (2006)

[6] MacChesney, J.B. & Guggenheim, H.J., Growth and electrical properties of vanadium dioxide containing selected impurity ions, *J. Phys. Chem. Solids* **30**, 225 - 234 (1969)

[7] Lopez, R., Feldman, L.C. & Haglund, R.F. 2005 Size dependent optical properties of VO_2 nanoparticle arrays *Phys. Rev. Lett.* **93,** 177403 (2005)

[8] Qazilbash, M.M., Burch K.S., Whisler, D., Shrekenhamer, D., Chae, B.G., Kim, H.T., & Basov, D.N., Correlated metallic state of vanadium dioxide, *Phys. Rev. B* **74** 205118 (2006)

[9] Becker, M.F., Buckman, A.B., Walser, R.M., Lepine, T., Georges, P. & Brun, A., Femtosecond Laser Excitation of the Semiconductor-Metal Phase Transition in VO_2, *Appl. Phys. Lett.* **65**, pp.1507-1509 (1994)

[10] Rini, M., Cavelleri, A., Schoenlein, R. W., Lopez, R., Feldman, L. C., Haglund, R. F., Jr., Boatner, L. A. & Haynes, T. E., Photo-induced phase transition in VO_2 nanocrystals: ultrafast control of surface plasmon resonance, *Optics Letters* **30**, 558-560 (2005)

[11] Snoke, D., Coherent questions, *Nature (News and Views),* , **443**, 403 (2006)

[12] Eisenstein, J.P. & MacDonald, A.H., Bose-Einstein condensation of excitons in bilayer electron systems, *Nature* **432**, 691-694 (2004).

[13] Babulanam, S.M., Eriksson, T.S., Niklasson, G.A. & Granqvist, C. G., Thermochromic VO_2 films for energy-efficient windows, *Proc. SPIE - Materials and Optics for Solar Energy Conversion and Advanced Lighting Technology* **Vol. 692** 8-18 (1986)

[14] Biermann, S., Poteryaev, A., Lichtenstein, A.I. & Georges, A., Dynamical singlets and correlation-assisted Peierls transition in VO_2, Phys. Rev. Letts., 94, 026404(1-4) (2005).

[15] Kim, H., Chae, B., Youn, D., Maeng, S., Kim, G., Kang, K. & Lim, Y., Mechanism and observation of Mott transition in VO_2-based two- and three-terminal devices, New Journal of Physics 6, 52 (2004).

[16] Brassard, D., Fourmaux, S., Jean-Jacques, M. Keieffer, J.C. & El Khakani, M. A., Grain size effect on the semiconductor-metal phase transition characteristics of magnetron sputtered VO_2 thin films, Appl. Phys. Lett., 87, 051910 (1-3) (2005).

[17] Cavalleri, A., Rini, M., Chong, H. H.W., Fourmaux, S., Glover, T. E., Heimann, P.A., Kieffer, J.C. & Schoenlein, R.W., Band-Selective Measurements of Electron Dynamics in VO2 Using Femtosecond Near-Edge X-Ray Absorption, *Phys. Rev. Lett.* **95,** 067405 (2005).